Available online at www.sciencedirect.com
SCIENCE DIRECT®
C. R. Chimie 8 (2005) 1743–1749
COMPTES RENDUS CHIMIE
http://france.elsevier.com/direct/CRAS2C/

Full paper / Mémoire

'Chimie douce' synthesis, crystal and electronic structures of the novel $Hg_{\sim 4.2}Mo_{15}X_{19}$ (X = S, Se) compounds containing Hg_3, Mo_6 and Mo_9 clusters

Diala Salloum [a], Patrick Gougeon [a,*], Michel Potel [a], Régis Gautier [b]

[a] *Laboratoire de chimie du solide et inorganique moléculaire, UMR CNRS 6511, université Rennes-1, Institut de chimie de Rennes, avenue du Général-Leclerc, 35042 Rennes cedex, France*

[b] *Laboratoire de physicochimie, UMR CNRS 6511, École nationale supérieure de chimie de Rennes, Institut de chimie de Rennes, campus de Beaulieu, 35700 Rennes, France*

Received 31 August 2004; accepted after revision 18 January 2005

Available online 13 June 2005

Abstract

The new compounds $Hg_{\sim 4.2}Mo_{15}X_{19}$ (X = S, Se) were obtained by inserting mercury into the metastable $Mo_{15}X_{19}$ compounds at low temperature. Their crystal structures, determined from single-crystal X-ray diffraction data, show that the molybdenum–chalcogenide network is maintained through the synthesis. It consists of an equal mixture of $Mo_6X_8X_6$ and $Mo_9X_{11}X_6$ cluster units interconnected through Mo–X bonds as in the parent compounds. In both compounds, the mercury is present either as Hg^{2+} cations or forming linear clusters Hg_3^{2+}. It is the first time that the latter cluster is observed in a chalcogen environment. ***To cite this article: D. Salloum et al., C. R. Chimie 8 (2005)***.

Résumé

Les nouveaux composés $Hg_{\sim 4.2}Mo_{15}X_{19}$ (X = S, Se) ont été obtenus par insertion de mercure à basse température dans les binaires métastables $Mo_{15}X_{19}$. Leurs structures cristallines, déterminées par diffraction des rayons X sur monocristal, montrent que le réseau molybdène–chalcogène est maintenu durant la synthèse. Il est constitué de motifs $Mo_6X_8X_6$ et $Mo_9X_{11}X_6$ en proportion égale et interconnectés entre eux par des liaisons Mo–X, comme dans les composés parents. Dans les deux composés, le mercure se présente, soit sous la forme cationique Hg^{2+}, soit formant des clusters linéaires Hg_3^{2+}. C'est la première fois qu'un tel cluster est observé dans un environnement de chalcogènes. ***Pour citer cet article : D. Salloum et al., C. R. Chimie 8 (2005)***.

Keywords: Soft chemistry; Molybdenum; Mercury; Cluster; Chalcogenide compounds; X-ray crystal structures

Mots clés : Chimie douce ; Molybdène ; Mercure ; Cluster ; Chalcogénures ; Structures cristallines par rayon X

* Corresponding author.
E-mail address: Patrick.Gougeon@univ-rennes1.fr (P. Gougeon).

1631-0748/$ - see front matter © 2005 Académie des sciences. Published by Elsevier SAS. All rights reserved.
doi:10.1016/j.crci.2005.02.027

1. Introduction

Inorganic compounds containing low-valent molybdenum are generally characterized by metal clusters of diverse sizes and geometries. In reduced molybdenum chalcogenides, the Mo clusters can accept a variable number of electrons (often called metallic electrons or ME) available for Mo–Mo bondings. The ME count, which govern the physical properties, can be modified through topotactic reduction–oxidation reactions at low temperatures. This is particularly well exemplified by the silver deinsertion from $Ag_{3.6}Mo_9Se_{11}$ that yield the isomorphous metastable compound o-Mo_9Se_{11} [1]. The latter phase is a superconductor with 32 ME per Mo_9 cluster while the parent ternary compound is a semiconductor and have 35.6 ME per Mo_9. Previous works have shown that the indium molybdenum cluster chalcogenides such as $InMo_6S_8$, $In_{3.7}Mo_{15}S_{19}$, $In_{3.3}Mo_{15}Se_{19}$, $In_2Mo_{15}Se_{19}$ or $In_2Mo_6Se_6$ are also good candidates for topotactic reduction–oxidation reactions at low temperatures [2–6]. Indeed, the indium can be removed easily from the latter ternary compounds by oxidation with I_2 or HCl gas to give the corresponding metastable binary compounds. From the binaries thus obtained, new ternary phases can synthesized by electrochemical reactions or by low temperature diffusion of metals having low melting point [3]. By using the latter technique we could prepare the new mercury molybdenum chalcogenides $Hg_{\sim 4.2}Mo_{15}X_{19}$ (X = S, Se), the syntheses and crystal and electronic structures of which are described in this paper.

2. Experimental section

2.1. Syntheses

The compounds $Hg_{\sim 4.2}Mo_{15}X_{19}$ (X = S, Se) were obtained in three steps. The first one was the synthesis of the solid-state compounds $In_{3.7}Mo_{15}S_{19}$ and $In_{3.3}Mo_{15}Se_{19}$ then the obtaining of the binaries $Mo_{15}X_{19}$ (X = S, Se) by 'chimie douce' and, finally the synthesis of the title compounds by inserting mercury into the $Mo_{15}X_{19}$ compounds at low temperature. All these steps were performed on single-crystals.

2.1.1. $In_{3.7}Mo_{15}S_{19}$ and $In_{3.3}Mo_{15}Se_{19}$

Starting materials used for the synthesis of $In_{3.7}Mo_{15}S_{19}$ were MoS_2, In_2S_3 and Mo, all in powder form. For $In_{3.3}Mo_{15}Se_{19}$, the initial products were $MoSe_2$, InSe and Mo. Before use, Mo powder was reduced under H_2 flowing gas at 1000 °C during 10 h in order to eliminate any trace of oxygen. The molybdenum disulfide and diselenide were prepared by the reaction of sulfur and selenium, respectively, with H_2 reduced Mo in a ratio 2:1 in an evacuated (ca. 10^{-2} Pa Ar residual pressure) and flame-baked silica ampoule, heated at 800 °C during 2 days. The indium sesquisulfide was obtained by heating at 800 °C stoichiometric amounts of indium metal and sulfur powder in an evacuated sealed silica ampoule. InSe was synthesized from indium and selenium shots heated at 450 °C in an evacuated sealed silica ampoule. All starting reagents were found monophasic on the basis of their powder X-ray diffraction diagram recorded with an Inel curve sensitive position detector CPS 120 using Cu $K\alpha_1$ radiation. In order to avoid any contamination by oxygen and moisture, the starting reagents were mixed, ground together in a mortar and then cold-pressed in a purified argon-filled glove box. The pellets (ca. 3 g) of the starting reagents were then loaded in molybdenum crucibles (depth: 2.5 cm; diam.: 1.5 cm), which were previously cleaned by heating at about 1500 °C in a high frequency furnace for 15 min under a dynamic vacuum of about 10^{-3} Pa and then sealed under a low argon pressure (300 h Pa) using an arc welding system. For $In_{3.7}Mo_{15}S_{19}$, the molybdenum crucible was heated at a rate of 50 °C h^{-1} up to 1120 °C and held there for 48 h, then cooled at 100 °C h^{-1} to 1000 °C and finally cooled down to room temperature in the furnace. For the selenide, the temperature of reaction was 1300 °C. The resulting products were black and air-stable and were found as pure phases on the basis of their X-ray powder diffraction diagram.

2.1.2. $Mo_{15}S_{19}$ and $Mo_{15}Se_{19}$

Single-crystals of the binary compounds were obtained from oxidation of single-crystals of $In_{3.7}Mo_{15}S_{19}$ and $In_{3.3}Mo_{15}Se_{19}$ by iodine in silica tube sealed under vacuum.

The end of the tube containing the crystals of the indium compounds and an excess of iodine was placed in a furnace with about 3 cm of the other end sticking out of the furnace, at about room temperature. The furnace was then heated at 300 °C for 96 h. At the end of the reaction, crystals of InI_3 and I_2 were obtained at the cool end of the tube.

2.1.3. $Hg_{\sim 4.2}Mo_{15}X_{19}$ (X = S, Se)

The mercury ternary phases were prepared by diffusion of mercury into crystals of $Mo_{15}X_{19}$ in silica tube sealed under vacuum at 400 °C during 96 h. In both cases, an excess of mercury was used.

2.2. Single-crystal X-ray studies

The X-ray diffraction data were collected on an Nonius Kappa CCD diffractometer using graphite-monochromated Mo–Kα radiation (λ = 0.71073 Å). The COLLECT program package [7] was employed to establish the angular scan conditions (ϕ and ω scans) used in the data collections. The data sets were processed using EvalCCD [8] for the integration procedure. For both crystals, an absorption correction was applied using the description of the crystal faces and the analytical method described by de Meulenaar and Tompa [9]. The structures were refined using SHELXL-97 [10]. The positions of the Mo and S atoms in $In_{3.7}Mo_{15}S_{19}$ [2] were used in the first stage of the refinement. The Hg positions were revealed by subsequent difference Fourier syntheses. Refinement of the occupancy factor of the Hg3 atoms led to the following stoichiometries: $Hg_{4.145(6)}Mo_{15}S_{19}$ and $Hg_{4.278(6)}Mo_{15}Se_{19}$. Relevant crystallographic data are listed in Table 1, and selected bond distances are given in Table 2.

Table 1
X-ray crystallographic and experimental data for $Hg_{4.145}Mo_{15}S_{19}$, and $Hg_{4.278}Mo_{15}Se_{19}$

Formula	$Hg_{4.145}Mo_{15}S_{19}$	$Hg_{4.278}Mo_{15}Se_{19}$
Formula weight (g mol^{-1})	2879.90	3796.86
Space group	$P6_3/m$	$P6_3/m$
a (Å)	9.5368(1)	9.8856(2)
c (Å)	18.5673(3)	19.2059(3)
Z	2	2
V (Å^3)	1462.46(3)	1625.44(5)
ρ_{calcd} (g cm^{-3})	6.473	7.745
T (°C)	20	20
λ (Å)	0.71073	0.71073
μ (mm^{-1})	29.190	46.636
R_1[a]	0.0426	0.0493
wR_2[b]	0.1027	0.1112

[a] $R_1 = \Sigma||F_o|-|F_c||/\Sigma|F_o|$.
[b] $wR_2 = \{\Sigma[w(F^2_o-F^2_c)^2]/\Sigma[w(F^2_o)^2]\}^{1/2}$.

Table 2
Selected interatomic distances for $Hg_{4.145}Mo_{15}S_{19}$, and $Hg_{4.278}Mo_{15}Se_{19}$

	$Hg_{4.145}Mo_{15}S_{19}$	$Hg_{4.278}Mo_{15}Se_{19}$
Mo1–Mo1 (×2)	2.6910(4)	2.6871(14)
Mo1–Mo1 (×2)	2.7182(5)	2.7100(8)
Mo2–Mo2 (×2)	2.6819(4)	2.6714(12)
Mo2–Mo3	2.7123(4)	2.7200(8)
Mo2–Mo3	2.7493(5)	2.7674(9)
Mo3–Mo3 (×2)	2.7484(7)	2.7591(13)
Mo1–Mo2	3.2739(5)	3.4866(9)
Mo1–X1	2.4455(13)	2.5667(11)
Mo1–X1	2.4466(10)	2.5816(10)
Mo1–X1	2.4856(15)	2.6107(14)
Mo1–X2	2.4925(9)	2.6510(12)
Mo1–X4	2.4331(15)	2.5440(12)
Mo2–X1	2.5014(9)	2.6640(12)
Mo2–X2	2.4769(13)	2.6102(10)
Mo2–X2	2.4374(15)	2.5736(10)
Mo2–X3	2.5760(6)	2.6665(10)
Mo2–X5	2.4127(13)	2.5338(11)
Mo3–X2 (×2)	2.4442(11)	2.5930(8)
Mo3–X3	2.4518(13)	2.574(2)
Mo3–X3	2.4570(12)	2.574(2)
Hg1–X1 (×3)	3.3218(7)	3.4211(10)
Hg1–X2 (×3)	3.2035(12)	3.2485(10)
Hg1–X5	2.5618(17)	2.6974(13)
Hg2–X3 (×3)	3.5129(15)	3.6247(9)
Hg2–X2 (×6)	3.7953(11)	3.8857(9)
Hg3–X2 (×2)	2.7369(11)	2.7124(11)
Hg3–X3	2.4276(13)	2.561(2)
Hg3–X4 (×2)	2.7403(14)	2.9577(14)
Hg1–Hg2 (×2)	2.6356(3)	2.6441(6)

2.3. Theoretical calculations

Calculations have been carried out within the extended Hückel formalism [11,12] with the program YAeHMOP [13]. The exponents (ξ) and the valence shell ionization potentials (H_{ii} in eV) were (respectively): 1.817, –20.0 for S 3 s; 1.817, –13.3 for S 3p; 1.956, –8.34 for Mo 5 s; 1.921, –5.24 for Mo 5p; 2.649, –13.68 for Hg 6 s; 2.631, –8.47 for Hg 6p. H_{ii} values for Mo 4d and Hg 5d were set equal to –10.50 and –17.50, respectively. Linear combination of two Slater-type orbitals of exponents $\zeta_1 = 4.542$ and $\zeta_2 = 1.901$ with the weighting coefficients $c_1 = c_2 = 0.5898$, and $\zeta_1 = 6.436$ and $\zeta_2 = 3.032$ with the weighting coefficients $c_1 = 0.6438$ and $c_2 = 0.5215$ were used to represent the Mo 4d and Hg 5d atomic orbitals, respectively. The density of states (DOS) and Crystal

Orbital Overlap Populations (COOP) were obtained using a set of 18 *k* points.

2.4. Magnetic measurements

The magnetic susceptibility was measured using a SQUID magnetometer (MPMS-XL, Quantum Design).

3. Results and discussion

3.1. Crystal and electronic structures

A view of the crystal structure of $Hg_{4.15}Mo_{15}S_{19}$ is shown in Fig. 1 as example. The molybdenum-chalcogen frameworks of the $Hg_{\sim 4.2}Mo_{15}X_{19}$ (X = S, Se) compounds are similar to those of the parent compounds $In_{3.7}Mo_{15}S_{19}$ and $In_{3.3}Mo_{15}Se_{19}$. They consist of an equal mixture of $Mo_6X^{i}_{8}X^{a}_{6}$ and $Mo_9X^{i}_{11}X^{a}_{6}$ (X = S, Se) cluster units linked through interunit Mo–X bonds (Fig. 2). The first unit is similar to that encoun-

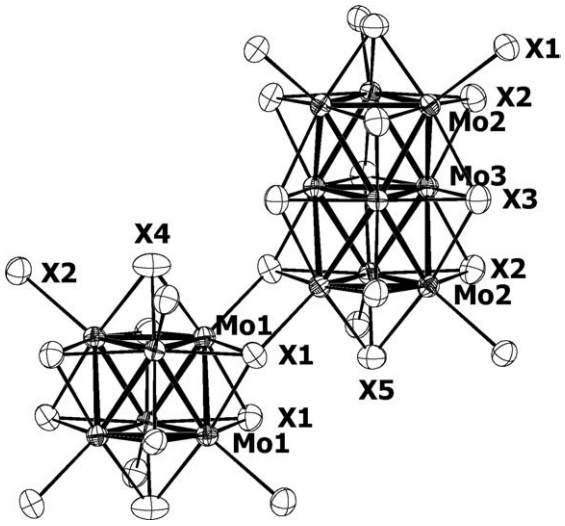

Fig. 2. The $Mo_6S_8S_6$ and $Mo_9S_{11}S_6$ units.

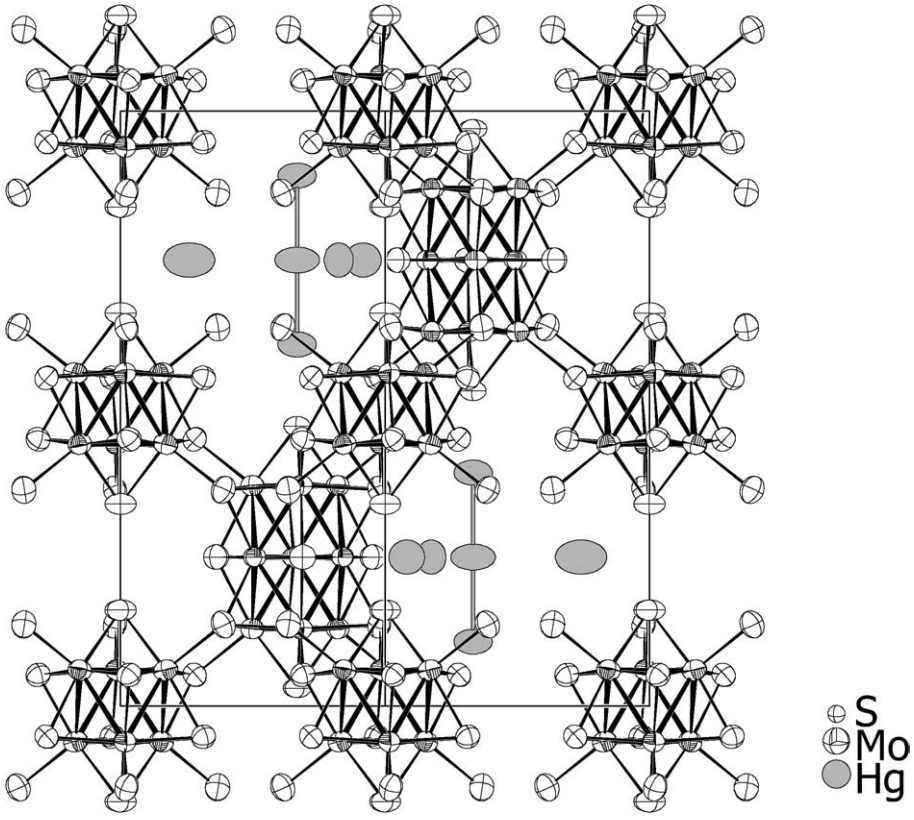

Fig. 1. View of the crystal structure of $Hg_{4.145}Mo_{15}S_{19}$, (97% probability ellipsoids).

tered in the ternary molybdenum chalcogenides $M_xMo_6X_8$ (M = Na, K, Ca, Sr, Ba, Sn, Pb, rare earth metal, 3d element; X = S, Se or Te), known as Chevrel phases. It corresponds to an Mo_6 octahedron surrounded by 8 face-capping inner X^i (6 X1 and 2 X4) and 6 apical X^a (X2) ligands. The Mo_9 core of the second unit results from the face sharing of 2 octahedral Mo_6 clusters. The Mo_9 cluster is surrounded by 11 X^i (6 X2, 3 X3 and 2 X5) atoms capping the faces of the bioctahedron and 6 apical X^a (X1) ligands above the ending Mo atoms. In the sulfide compound, the Mo–Mo distances within the Mo_6 clusters are 2.6910(4) Å (2.6871(14) in the selenide) for the intra-triangle distances (distances within the Mo_3 triangles formed by the Mo atoms related through the threefold axis) and 2.7182(5) Å (2.7100(8) in the selenide) for the inter-triangle distances. The Mo–Mo distances within the Mo_9 clusters are 2.6819(4) and 2.7484(7) Å (2.6714(12) and 2.7591(13) Å in the selenide) for the intra-triangle distances between the Mo2 and Mo3 atoms, respectively, and 2.7123(4) and 2.7493(5) Å (2.7200(8) and 2.7674(9) Å in the selenide) for those between the Mo_3 triangles. The $Mo_6X^i_8X^a_6$ and $Mo_9X^i_{11}X^a_6$ units are centered at 2b and 2c positions and have the point-group symmetry $\bar{3}$ and 3/*m*, respectively. The chalcogen atoms bridge either one (X1, X2, X4 and X5) or two (X3) Mo triangular faces of the clusters. Moreover the chalcogens X1 and X2 are linked to a Mo atom of a neighboring cluster. The Mo–X bond distances range from 2.4167(11) to 2.5032(14) Å within the Mo_6X_8 unit and from 2.3908(8) to 2.6262(11) Å within the Mo_9X_{11}. Each $Mo_9X^i_{11}X^a_6$ unit is interconnected to 6 $Mo_6X^i_8X^a_6$ units (and vice-versa) via interunit Mo1–X2 bonds (respectively, Mo2–X1) (Fig. 2) to form the three-dimensional Mo–X framework, the connectivity formula of which is $Mo_9X^i_5X^{i\text{-}a}_{6/2}X^{a\text{-}i}_{6/2}Mo_6X^i_2X^{i\text{-}a}_{6/2}X^{a\text{-}i}_{6/2}$. It results from this arrangement that the shortest intercluster Mo1–Mo2 distance between the Mo_6 and Mo_9 clusters is 3.2739(5) Å in the sulfide and 3.4866(9) Å in the selenide, indicating only weak metal–metal interaction.

In both compounds, the mercury is present either as Hg^{2+} cations (ie Hg3) or forming linear trinuclear clusters Hg_3^{2+}units (i-.e. Hg1 and Hg2) (Fig. 3). The Hg^{2+} cations occupy the sites in which the In^{3+} cations are located in the indium parent compounds (Fig. 3). The latter position corresponds to a triangular group of distorted octahedral cavities around the threefold axis, which are formed by two Mo_6X_8 and three Mo_9X_{11} units. These cavities are only partially occupied with 1.145(6) and 1.278(6) Hg^{2+} cations per triangular group for the sulfide and selenide compounds, respectively. The Hg3–S distances range from 2.4276(13) to 2.7403(14) Å and, the Hg3–Se ones from 2.561(2) to 2.9577(14) Å.

The Hg_3^{2+} cluster, which is for the first time observed in a chalcogen environment, resides in the two large cavities that are occupied by the monovalent indium cations related through the mirror plane in $In_{3.7}Mo_{15}S_{19}$ and $In_{3.3}Mo_{15}Se_{19}$. The Hg_3^{2+} cluster is linear and centrosymmetrical with Hg1–Hg2 distances of 2.6356(3) Å in the sulfide and 2.6441(6) Å in the selenide (Fig. 4). The latter distances are somewhat longer that those observed in the other inorganic compounds such as $Hg_3(AsF_6)_2$ [14], $Hg_3(AlCl_4)_2$ [15], $Hg_3(NbF_5)_2(SO_4)_2$

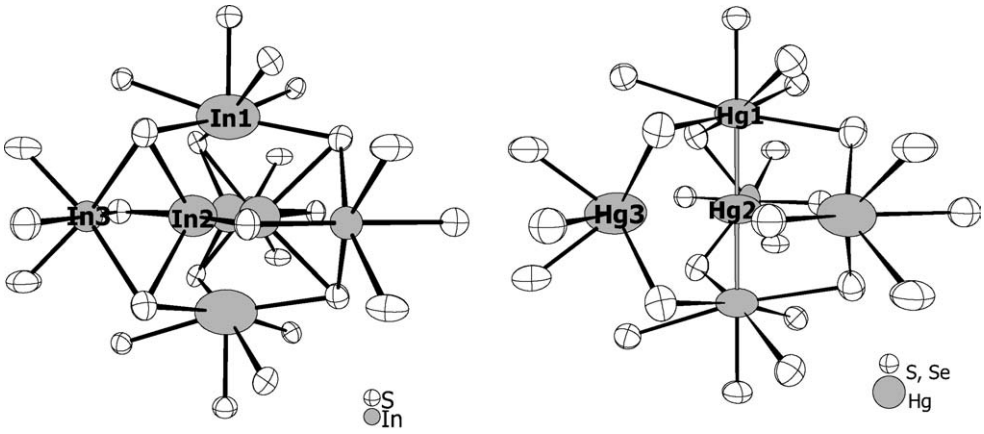

Fig. 3. Views of the In and Hg sites in $In_{3.7}Mo_{15}S_{19}$, (left) and $Hg_{\sim 4.2}Mo_{15}X_{19}$ (right).

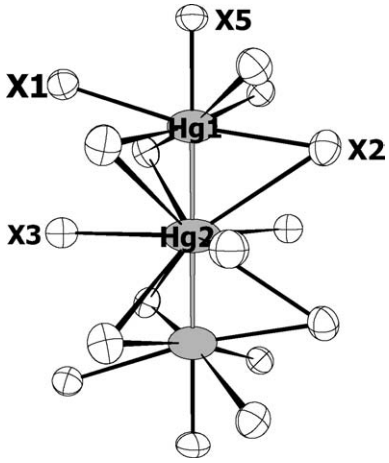

Fig. 4. The Hg_3 cluster with its chalcogen environment.

[16] and $Hg_3(TaF_5)_2(SO_4)_2$ [17] containing quasi- or linear Hg_3^{2+} groups in which the Hg–Hg distances range from 2.551 to 2.562 Å. The coordination environment about the mercury atoms is also different. The environment of the terminal mercury atoms Hg1 is similar to that of the monovalent indium cations and thus consists of seven chalcogen atoms. The Hg1–X distances range from 2.5618(17) to 3.3218(7) Å in the sulfide and, from 2.6974(13) to 3.421(1) Å in the selenide. The shortest Hg1–X5 bond is collinear with the Hg–Hg bonds and is, most likely, covalent in character. The central mercury atoms Hg2 is surrounded by nine chalcogen atoms forming a tricapped trigonal prism. The distances between the Hg2 mercury and the capping chalcogen atoms are 3.5129(15) Å and 3.6247(9) Å for the sulfide and selenide, respectively, while the other distances between Hg2 and the chalcogens forming the trigonal prism are 3.7953(11) and 3.8857(9), respectively. Hg1–Hg2 distances are consistent with the presence of metal–metal bonding in the Hg_3 unit. The expected metallic electron (ME) count for linear Hg_3–X_2 units with two metal–metal bonds is 34 [17]. Such a ME count induces a + 2 charge on the Hg_3 cluster. This oxidation state is also the one observed for the Hg_3 clusters present in the inorganic compounds mentioned above. Considering Hg^{2+} and Hg_3^{2+} cations in the title compound, the total ME count of Mo_6 and Mo_9 clusters is equal to 56.4. Previous theoretical studies have shown that optimal ME counts, i.e. complete filling of Mo–Mo bonding and non-bonding levels separated from Mo–Mo antibonding levels by a significant energy gap, are equal to 24 and 36 for such Mo_6 and Mo_9 clusters, respectively [18,19]. Assuming weak interaction between the clusters in the solid-state structure, band structure of the title compound showing a significant energy gap for the ME count of 24 + 36 = 60 is expected. Total and Mo_9 projected density of states (DOS) sketched in Fig. 5 were computed for the model compound $Hg_4Mo_{15}S_{19}$ where only one of the three Hg3 equivalent crystallographic position is occupied. The Fermi level for the ME count of 56 (that corresponds to the presence of four Hg atoms in the unit cell) cuts a narrow peak of DOS mainly centered on d orbitals of the Mo_6 cluster. Metallic properties can be envisioned for the title compound. This was confirmed by magnetic susceptibility measurements that were carried out on batches of single-crystals of about 100 mg in an applied field of 20 Oe using a dc SQUID magnetometer. Indeed, $Hg_{4.145}Mo_{15}S_{19}$ and $Hg_{4.278}Mo_{15}Se_{19}$ show a diamagnetic shielding signal below 4 K indicating a superconducting transition. Finally, it should be mentioned that a band gap of 0.20 eV separating overall Mo–Mo bonding and non-bonding bands from Mo–Mo antibonding bands is reached for the ME count of 60. Such an electron count would render the material semiconducting through suitable doping. Indeed, Mo–Mo and Mo–S overlap populations hardly change overall upon additions of elec-

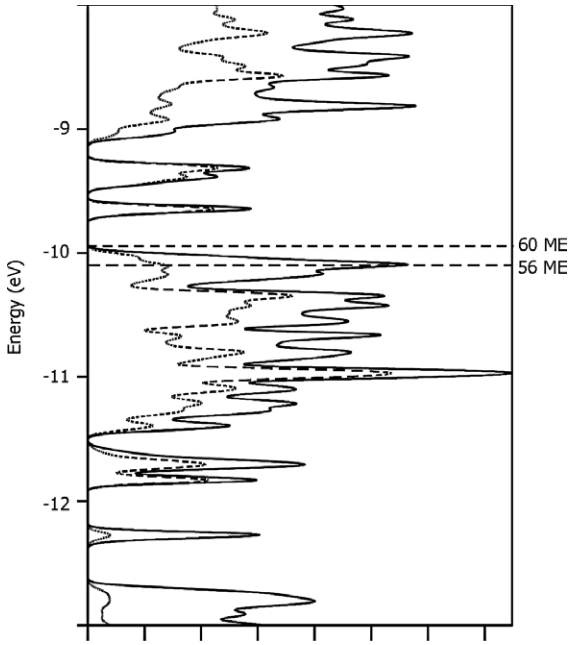

Fig. 5. EHTB calculations for $Hg_4Mo_{15}S_{19}$: total density of states (plain) and Mo_9 contribution (dotted).

trons. Analyses of the COOP (not shown here) indicate that the intercluster Mo1–Mo2 and intra Mo_9 cluster Mo3–Mo3 should slightly lengthen, as well as Mo–S distances, whereas other Mo–Mo bonds of Mo_6 and Mo_9 units should slightly shorten when electrons are added.

4. Supplementary material

Further details of the crystal structure investigation may be obtained from the Fachinformationszentrum Karlsruhe, D-76344 Eggenstein-Leopoldshafen, Germany (fax: +49 7247 808 666; e-mail: crysdata@fiz-karlsruhe.de), on quoting the depository number CSD-414276 and CSD-414277.

References

[1] P. Gougeon, M. Potel, J. Padiou, M. Sergent, C. Boulanger, J.-M. Lecuire, J. Solid-State Chem. 71 (1987) 543.
[2] D. Salloum, R. Gautier, P. Gougeon, M. Potel, J. Solid-State Chem. 177 (2004) 1672.
[3] M. Potel, P. Gougeon, R. Chevrel, M. Sergent, Rev. Chim. Miner. 21 (1984) 509.
[4] B.D. Davis, W.R.J. Robinson, Solid-State Chem. 85 (1990) 332.
[5] J.M. Tarascon, G.W. Hull, Mater. Res. Bull. 21 (1986) 859.
[6] J.M. Tarascon, Solid-State Ionics 18 (1986) 768.
[7] B.V. Nonius, COLLECT, data collection software, Nonius BV, 1999.
[8] A.J.M. Duisenberg, Reflections on Area Detectors, Ph.D. thesis, Utrecht, The Netherlands, 1998.
[9] J. de Meulenaar, H. Tompa, Acta Crystallogr. A19 (1965) 1014–1018.
[10] G.M. Sheldrick, Programs for Crystal Structure Analysis (Release 97-2). Institüt für Anorganische Chemie der Universität, Tammanstrasse 4, D-3400 Göttingen, Germany, 1998.
[11] R. Hoffmann, J. Chem. Phys. 39 (1963) 1397.
[12] M.-H. Whangbo, R. Hoffmann, J. Am. Chem. Soc. 100 (1978) 6093.
[13] G.A. Landrum, YAeHMOP, Yet Another extended Hückel Molecular Orbital Package, Ithaca, NY, 1997 (release 2.0).
[14] B.D. Cutforth, C.G. Davies, P.A.W. Dean, R.J. Gillespie, P.R. Ireland, P.K. Ummat, Inorg. Chem. 12 (1973) 1343.
[15] R.D. Ellison, H.A. Levy, K.W. Fung, Inorg. Chem. 11 (1972) 833.
[16] I.D. Brown, R.J. Gillespie, K.R. Morgan, J.F. Sawyer, K.J. Schmidt, Z. Tun, P.K. Ummat, J.E. Vekris, Inorg. Chem. 26 (1987) 689.
[17] T.A. Albright, J.K. Burdett, M.-H. Whangbo, in: Orbital Interactions in Chemistry, Wiley, New York, 1985 , p. 258.
[18] T. Hughbanks, R. Hoffmann, J. Am. Chem. Soc. 105 (1983) 1150.
[19] R. Gautier, P. Gougeon, J.-F. Halet, M. Potel, J.-Y. Saillard, J. Alloys Compds 262–263 (1997) 311.